

PREDICTION EQUATIONS FOR CREEP AND DRYING SHRINKAGE IN CONCRETE OF WIDE-RANGING STRENGTH

(Translation from Proceedings of JSCE, No.690/V-53, November 2001)



Kenji SAKATA



Tatsuya TSUBAKI



Shoichi INOUE



Toshiki AYANO

As the performance of concrete is enhanced and high-strength concrete comes into common use, the model code for concrete is being improved to cope with the changes. Today, prediction equations for creep and shrinkage in high-strength concrete are an essential part of the model code. In this study, the precision of current prediction equations is examined using a number of databases, from which data providing reliable knowledge of the effect of concrete strength on creep and shrinkage is extracted. New prediction equations are proposed, and this paper shows that they are very simple and applicable to a wide range of concrete strengths.

Keywords: *prediction equation, creep, drying shrinkage, high-strength concrete, data base*

K. Sakata, a professor in Environmental and Civil Engineering at Okayama University, Okayama, Japan, received his Doctor of Engineering degree from Kyoto University, Japan in 1976. His research interests include the prediction of concrete shrinkage, creep, and fatigue properties. He is a fellow of the JSCE.

T. Tsubaki is a Professor in the Department of Civil Engineering at Yokohama National University, Japan. He obtained his Ph.D. from Northwestern University in 1980. His research interests include the time-dependent mechanical behavior of concrete and the analysis of concrete structures. He is a member of the JSCE and the JCI.

S. Inoue is a Professor in the Department of Civil Engineering at Tottori university, Tottori, Japan. He received his Doctor of Engineering Degree from Kyoto University in 1985. His research interests include the fatigue properties, time-dependence deformation of concrete structures, and properties of fresh concrete. He is a member of the ACI, JSMS, JCI, LPC and JSCE.

T. Ayano, an associate professor in Environmental and Civil Engineering at Okayama University, Okayama, Japan, received his Doctor of Engineering degree from Okayama University in 1993. His research interests include the prediction of concrete shrinkage and creep. He is a member of the JSCE.

1. INTRODUCTION

Every increment in concrete creep and shrinkage strain increases the deflection of a concrete member, affects cracking progress, and causes loss of prestress. Thus, to check the safety, durability and serviceability of concrete structures, it is very important to have a means of predicting creep and shrinkage over the long term.

Higher strength concrete has now been used extensively, and research into high-performance concrete and its applications has been very active. The wide acceptability of high-performance concrete can be attributed to the establishment of a technique for producing high-performance concrete using silica fume and high-range water-reducing admixtures. Its use has led to the construction of slender, lightweight concrete members. Increasing the strength of concrete may also improve the durability and extend the service life of concrete structures. In this sense, many hope that high-performance concrete may decrease environmental loading. On the other hand, others point out that high-strength concrete is prone to cracking. Whatever one's perspective, however, it is very important to precisely predict both creep and shrinkage at the design stage in order to discuss the durability and service life of concrete structures.

Most model codes are based on prediction equations that consist of several factors relating to concrete creep and shrinkage [1][2]. Some existing codes are applicable to high-performance concrete. The Japan Society of Civil Engineers (JSCE) has its own prediction equations [3], but the model is proven only for normal-strength concrete up to 60 N/mm². It has not been clarified whether the model is available for high-strength concrete as well.

High-strength concrete with strength at 28 days exceeding 70 N/mm² is not unusual. Indeed, the 2002 edition of the Standard Specifications for Design and Construction of Concrete Structures cover concrete whose 28-day strength is up to 80 N/mm². Thus the requirement for creep and shrinkage prediction equations suitable for a wide range of concrete strengths is increasing.

Both RILEM and JSCE are establishing databases of creep and shrinkage. In this paper, new prediction equations that are simple and available for a wide range of strengths are proposed on the basis of data extracted from the RILEM and JSCE databases as well as other minor sources.

2. REPRESENTATIVE PREDITION EQUATIONS

2.1 Outline of data used

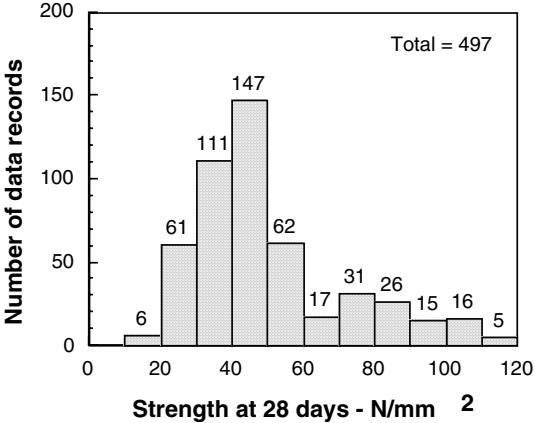
The main source of data used in establishing the new prediction equations was the creep and shrinkage data collected by RILEM and JSCE. The RILEM database holds data consisting of 512 creep records and 419 shrinkage records [4], while the JSCE database contains 259 creep records and 219 shrinkage records [5]. The RILEM database consists mainly of data from the western countries, while the JSCE has collected data from papers published by Japanese organizations.

Every data set was subjected to regression using the hyperbola expressed by Equation (1). The standard divisions of the optimal value of C_0 and C_1 were checked. If each of them was beyond 10, the data was judged to be unreliable and was excluded from use in the study.

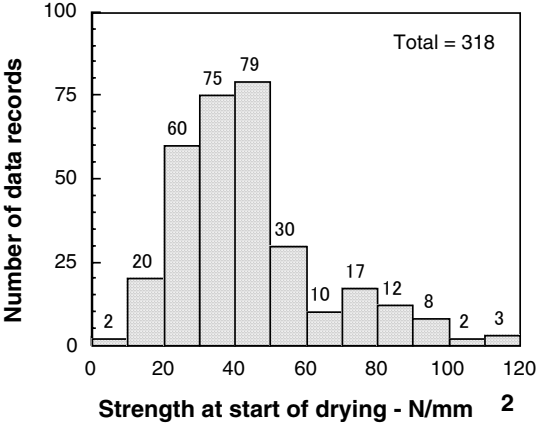
$$\text{Creep or shrinkage} = \frac{C_0 \cdot t}{C_1 + t} \quad (1)$$

In total, 295 creep records and 200 shrinkage records from the RILEM and JSCE database were selected for use in the study. Not all sets of shrinkage and creep data include all information. However, the selected data sets were obtained for concrete specimens with a wide range of strength and dimensions. Summaries of the selected drying shrinkage and creep data are shown

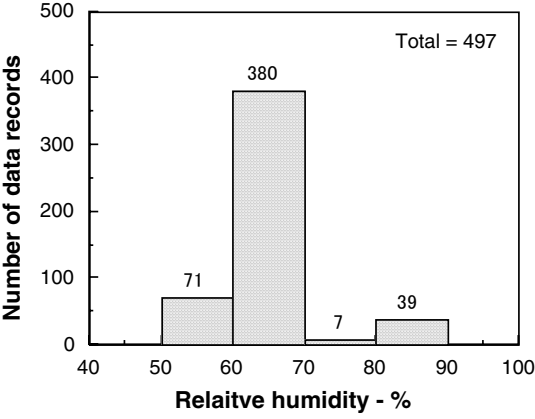
in Figures 1 and 2, respectively. All data was measured at 20°C. Drying shrinkage was obtained from unloaded specimens. The drying shrinkage strain of high-strength concrete was obtained by subtracting the strain of a sealed specimen from that of an unsealed specimen. In cases where the start of drying was more than one week after casting, the effect of autogenous shrinkage on the strain of unsealed specimens was regarded to be negligible. Creep strain was obtained by subtracting the strain of an unloaded specimen from that of a loaded specimen. The size and shape of specimens under loading and unloading were the same.



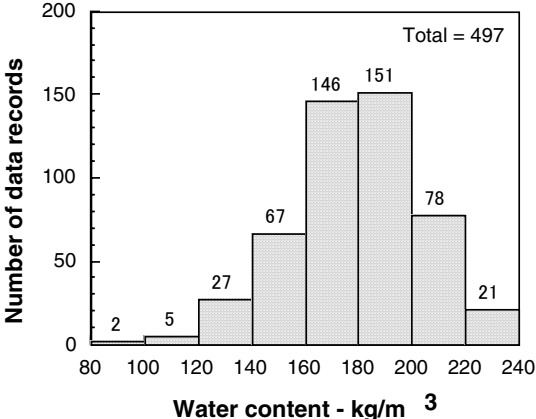
(a) Compressive strength at 28 days



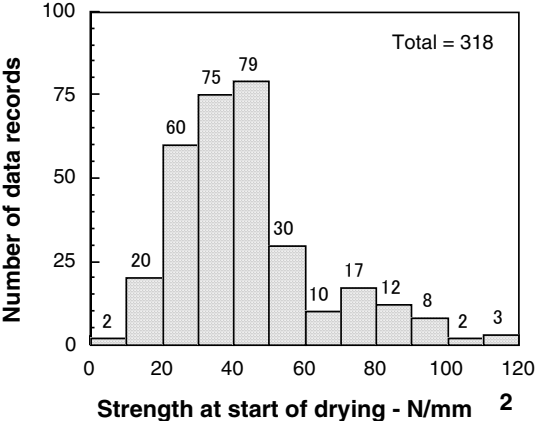
(b) Compressive strength at start of drying



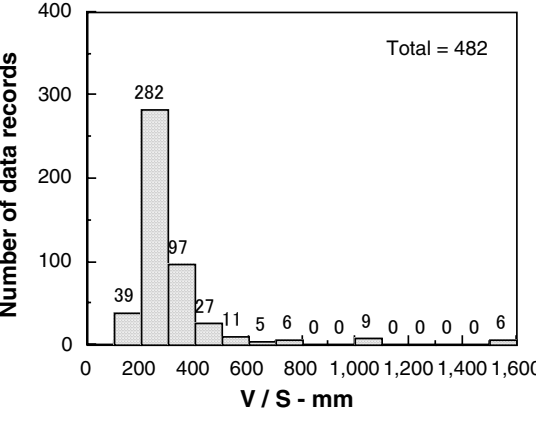
(c) Relative humidity at atmosphere



(d) Water content of Concrete

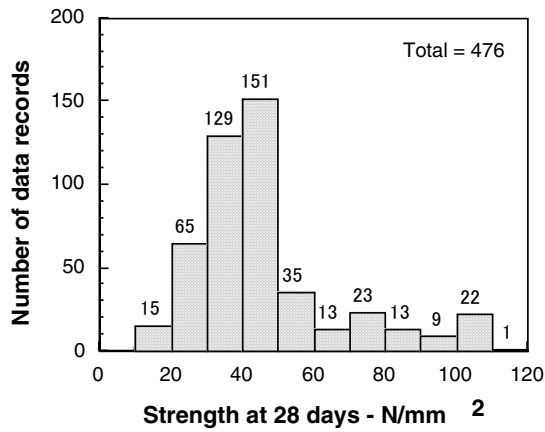


(e) Age at start of drying

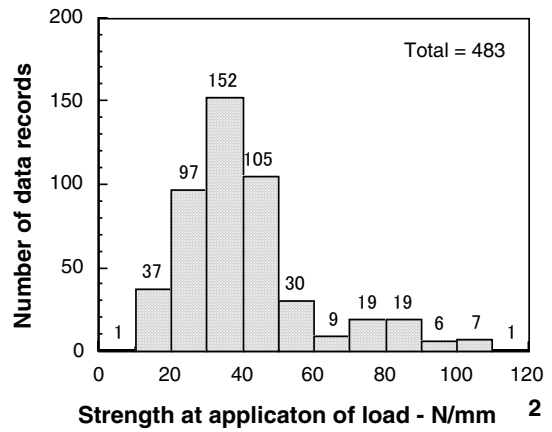


(f) Specimen size

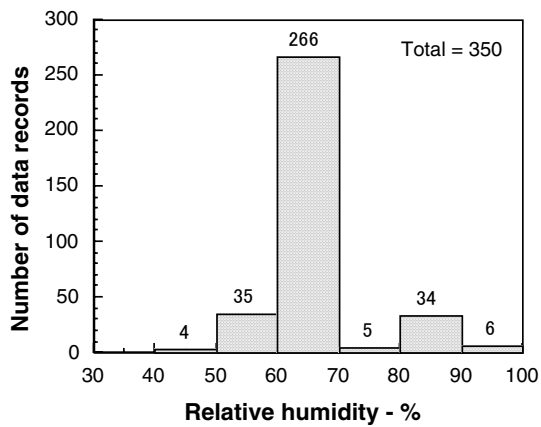
Figure 1 Summaries of data used for drying shrinkage



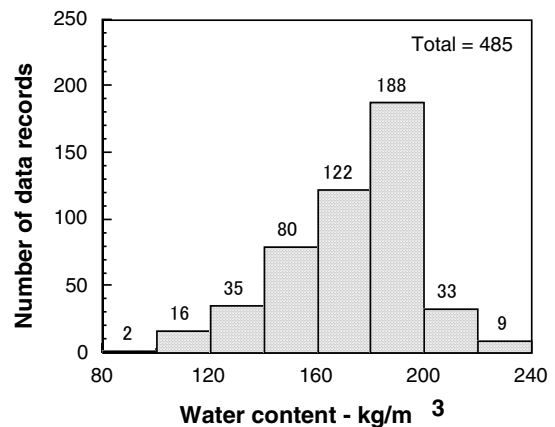
(a) Compressive strength at 28 days



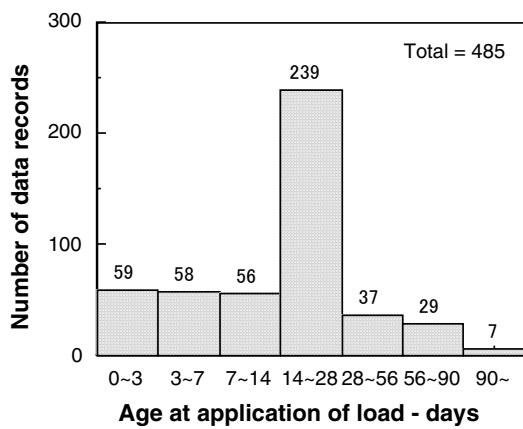
(b) Compressive strength at initial load application



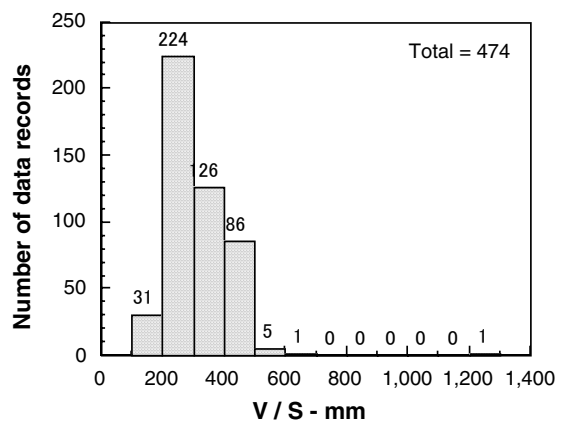
(c) Relative humidity of atmosphere



(d) Water content of concrete



(e) Age at initial load application of load



(f) Specimen size

Figure 2 Summaries of data used for creep

2.2 Applicable range of representative prediction equations

Table 1 shows the applicable range of the representative prediction equations for creep and shrinkage. Table 2 shows the factors needed to predict creep and shrinkage using each prediction equation, since the factors differ according to the equation selected. Model B3 [6] requires more factors than any of the other prediction equations listed in Table 1. As for creep, model B3 predicts the creep function $J(t, t')$; models CEB [7] and GZ [8] predict the creep coefficient; and the JSCE model [9] predicts specific creep $C(t, t')$. Furthermore, the creep coefficient $\phi_{28}(t, t')$ predicted by model CEB is the product of specific creep and Young's modulus at 28 days. The creep coefficient $\phi(t, t')$ predicted by model BZ is the product of specific creep and Young's modulus at the application of loading. When Young's modulus at the age of t' is represented by $E(t')$, the relationship between $J(t, t')$, $C(t, t')$, $\phi_{28}(t, t')$ and $\phi(t, t')$ is represented as follows:

$$\begin{aligned} J(t, t') &= \frac{1}{E(t')} + C(t, t') \\ &= \frac{1}{E(t')} + \frac{\phi_{28}(t, t')}{E(28)} = \frac{1}{E(t')} + \frac{\phi(t, t')}{E(t')} \end{aligned} \quad (2)$$

Where, t : current age (days), t' : age at first application of loading (days)

The accuracy of creep models CEB, BZ, and the JSCE model was examined by using the specific creep strain. The accuracy of model B3 was examined by using the creep function. In cases where Young's modulus was also available in the database, it was used to calculate specific creep strain. Otherwise, Young's modulus was calculated using the proposed equation in each model code including the creep and shrinkage model.

The factors used as the basis for prediction are listed in Table 3; these are values for ordinary concrete. Table 4 gives the predicted shrinkage strain and specific creep for each model based on these factors. The values predicted by the JSCE model are a little bigger than the others.

Table 1 Applicable range of each prediction equation.

	JSCE Model	Model CEB	Model B3	Model GZ
Strength at 28 days(N/mm ²)	Less than 70	20~90	17.2~68.95	20~68.95
Aggregate/cement ratio in weight	-	-	2.5~13.5	-
Unit cement content (kg/m ³)	260~500	-	160~721	-
Water-cement ratio	0.40~0.65	-	0.35~0.85	0~0.6
Relative humidity (%)	45~80	40~100	40~100	40~100
Type of Cement	Normal	Normal Low heat Rapid hardening High strength	Normal Low heat Rapid hardening High strength	Normal Low heat Rapid hardening High strength
Volume-surface ratio (mm)	100~300	-	-	-
t' and t_0	-	-	$t' \geq t_0$	≥ 2 days
Curing method	-	-	Autoclave Water curing Sealed curing	-

t' : Age at initial load application (days), t_0 : Age at start of drying (days)

Table 2 Necessary factors for each prediction equation

	JSCE Model		Model CEB		Model B3		Model GZ	
	Shrinkage	Creep	Shrinkage	Creep	Shrinkage	Creep	Shrinkage	Creep
Strength at 28 days			○	○	○	○		○
Strength at t' or t_0							○	○
Aggregate/cement						○		
Unit cement content		○				○		
Unit water content	○	○			○	○		
Water-cement ratio		○				○		
Relative humidity	○	○	○	○	○	○	○	○
Type of cement			○		○	○	○	
Start of drying	○				○	○		○
t'		○		○		○		○
Size of specimen	○	○	○	○	○	○	○	○
Shape of specimen					○	○		
Curing method					○	○		

t' : age at initial load application (days)

Table 3 Set values for prediction

Item	Input data
Start of drying	7 days
Age at initial load application	7 days
Relative humidity	60 %
Strength at 28 days	30 N/mm ²
Strength at initial load application	20 N/mm ²
Cement type	Normal
Aggregate-cement ratio	6
Unit cement ratio	300 kg/m ³
Unit water content	180 kg/m ³
Water-cement ratio	60 %
Size and shape of specimen	100 × 100 × 400 mm

Table 4 Predicted values

	JSCE Model	Model CEB	Model B3	Model GZ
Drying shrinkage (μ)	790	557	441	817
Specific creep ($\mu/(N/mm^2)$)	214	130	107	134

2.3 Accuracy of shrinkage prediction equations

Figure 3 presents a comparison between experimental shrinkage data extracted from the databases and the JSCE model predictions. Here, however, the 28-day concrete compressive strength is less than 80 N/mm². On the other hand, the comparison in Figure 4 is for concrete with

a 28-day compressive strength greater than 80 N/mm². The start of drying is indicated by ● and ○, representing 28 days and 1 day, respectively. As is clear from these figures, the JSCE model tends to predict larger values than the experimental data when the start of drying is late.

Figure 5 is a comparison between experimental shrinkage data and predictions by model CEB. Here, only data within the applicable range of model CEB was used for comparison. Model CEB is able to closely predict the experimental shrinkage data from the western database well. However, the predicted values are smaller than the data from the JSCE database. Figure 6 compares data outside the applicable range of model CEB. The 28-day strength expressed by ● is greater than 90 N/mm². Model CEB underestimates the shrinkage strain of this high-strength concrete.

Figure 7 is a comparison between experimental shrinkage data and predictions by model B3. Here, only data within the applicable range of model B3 was used for comparison. Model B3 tends to underestimate experimental shrinkage data, even within its applicable range. As is clear from Figure 8, which is a comparison with data outside its applicable range, model B3 underestimates concrete shrinkage especially significantly when the 28-day strength is greater than 70 N/mm². In this figure, data for concrete in this strength range is indicated by ●.

Figure 9 compares experimental shrinkage data and predictions by model GZ. Here again, only data within the applicable range of model GZ was used for comparison. The GZ model can predict experimental shrinkage strain to an accuracy of ±40% when the data is within its applicable range. On the other hand, Figure 10 is a comparison between predictions by model GZ and experimental shrinkage data beyond the applicable range of the model. Symbols ○ represent shrinkage data for concrete whose strength at 28 days is greater than 70 N/mm². Symbols □ represent concrete whose strength at 28 days is less than 20 N/mm². Shrinkage data for concrete whose start of drying is earlier than 2 days is shown by ●. Model GZ is able to predict the shrinkage strain of high-strength concrete. However, in the case of concrete whose start of drying is earlier than 2 days, the values predicted by model GZ are larger than the experimental values.

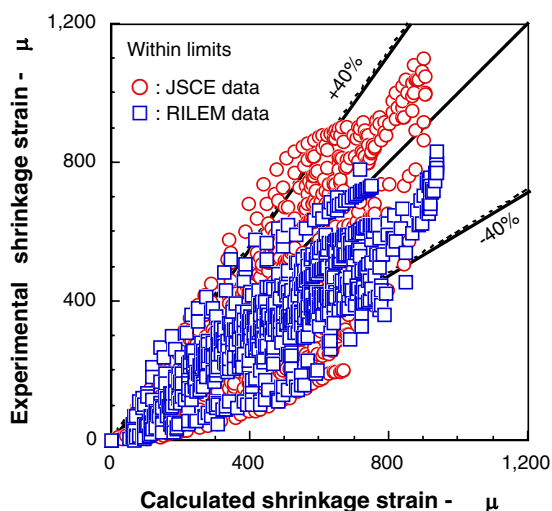


Figure 3 Precision of the JSCE Model

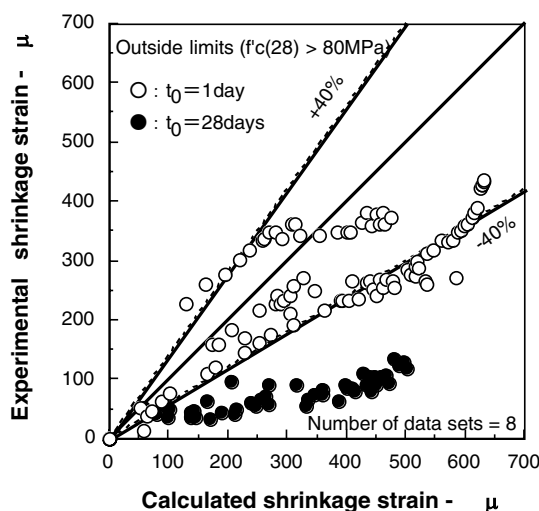


Figure 4 Precision of the JSCE Model

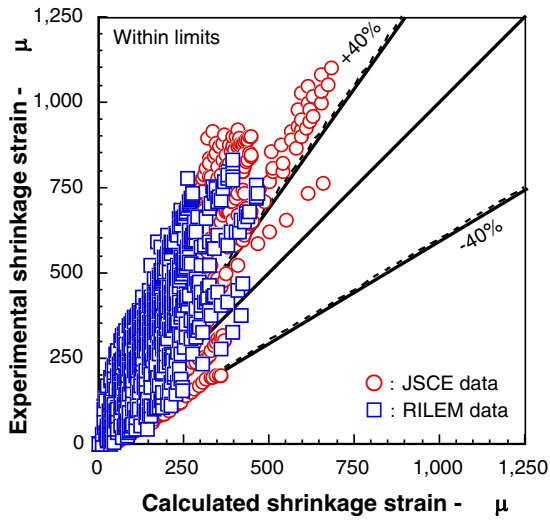


Figure 5 Precision of Model CEB

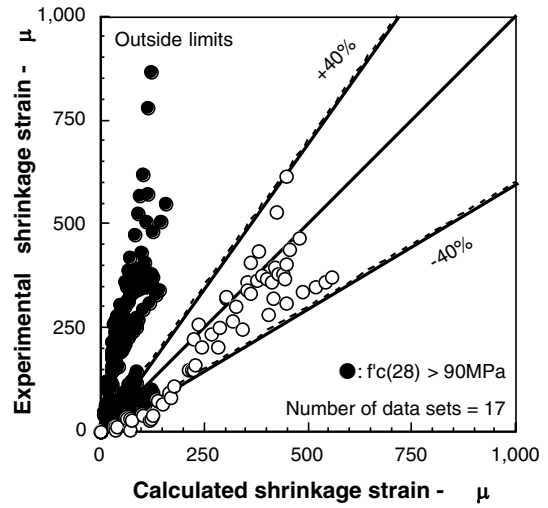


Figure 6 Precision of Model CEB

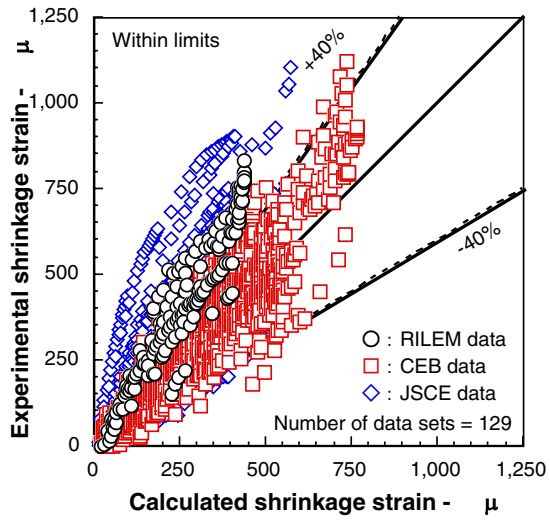


Figure 7 Precision of Model B3

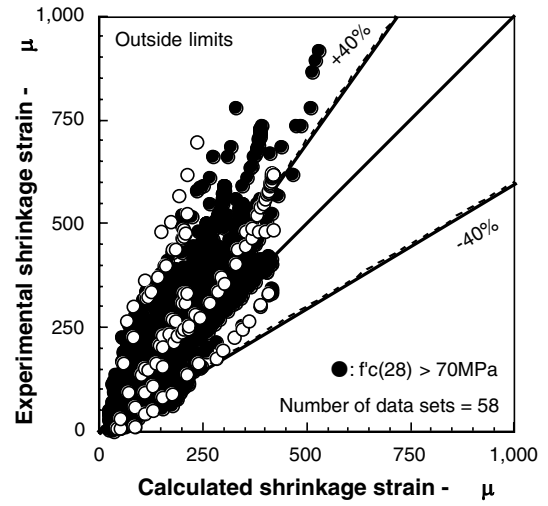


Figure 8 Precision of Model B3

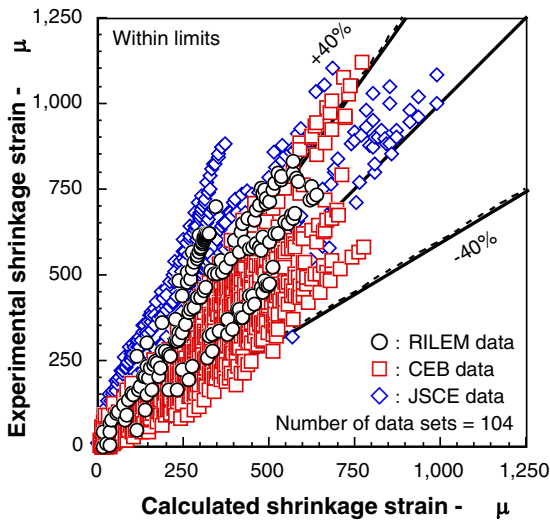


Figure 9 Precision of Model GZ

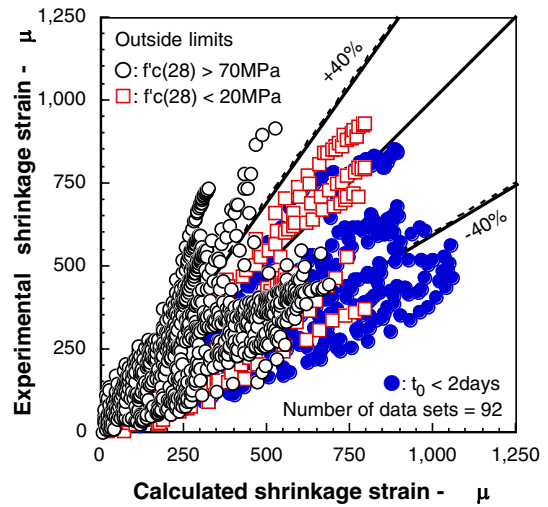


Figure 10 Precision of Model GZ

Each of the models described above is able to predict shrinkage strain reasonably well when the data is within its applicable range. However, out of this range, the capabilities of the models vary. The JSCE model overestimates shrinkage for high-strength concrete when the age at the start of drying is 28 days. On the other hand, predictions by the other models are smaller than the experimental values in the case of high-strength concrete. Thus, prediction equations used for normal-strength concrete cannot be applied as is to high-strength concrete.

2.4 Accuracy of creep prediction equations

Figure 11 is a comparison of experimental values of specific creep extracted from the databases and predictions by the JSCE model. The figure includes data for concrete whose 28-day strength is greater than 100 N/mm². Figure 12 shows a case where the predictions by the JSCE model are extremely unreasonable. The JSCE model takes account of factors representing the concrete mixture, specimen size, and environmental conditions. It does not include a strength factor. Even where other creep models that include a strength factor are able to predict creep well, the JSCE model sometimes gives unreasonable results.

Figure 13 compares the experimental specific creep strain with predictions by model CEB. Data within the applicable range of model CEB was used for the comparison. Figure 14 is a similar comparison but for data outside the applicable range of model CEB. As is clear from these figures, model CEB is able to predict creep well even outside the usual range.

Figure 15 compares experimental creep data with predictions data by model B3. Data within the applicable range of model B3 was used for comparison. The difference between experimental values and predictions appears large even within the applicable range. Figure 16 shows a similar comparison for data outside the applicable range of model B3. Here, data for concrete whose 28-day strength is greater than 70 N/mm² is indicated by ●. It is clear that model B3 is able to predict the creep of high-strength concrete with accuracy.

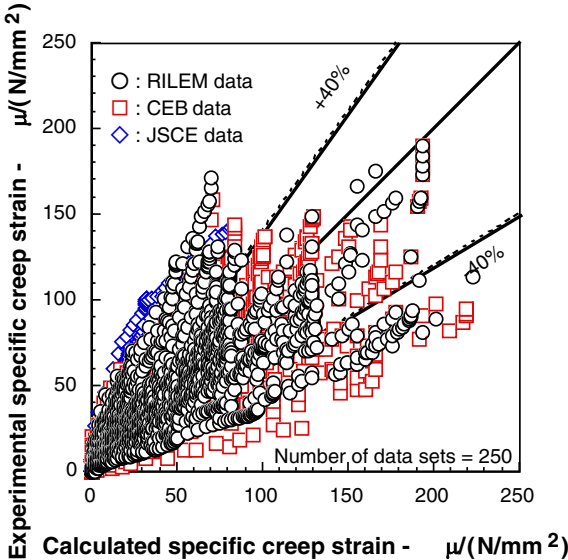


Figure 11 Precision of the JSCE Model

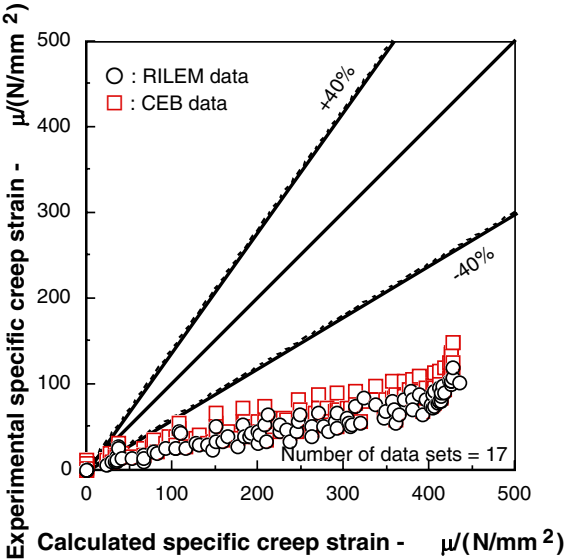


Figure 12 Precision of the JSCE Model

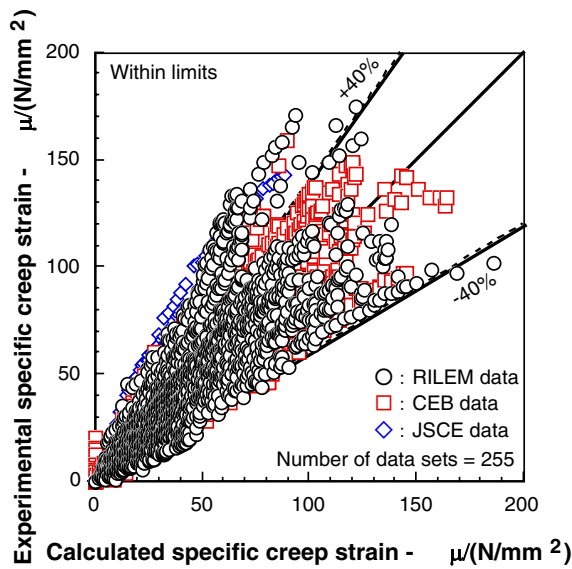


Figure 13 Precision of Model CEB

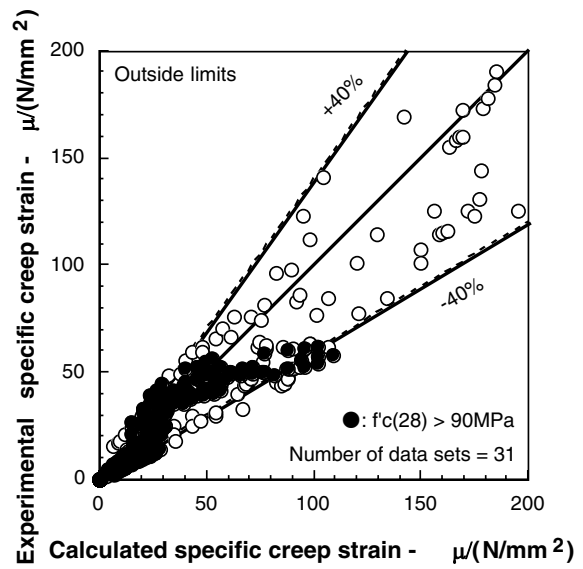


Figure 14 Precision of Model CEB

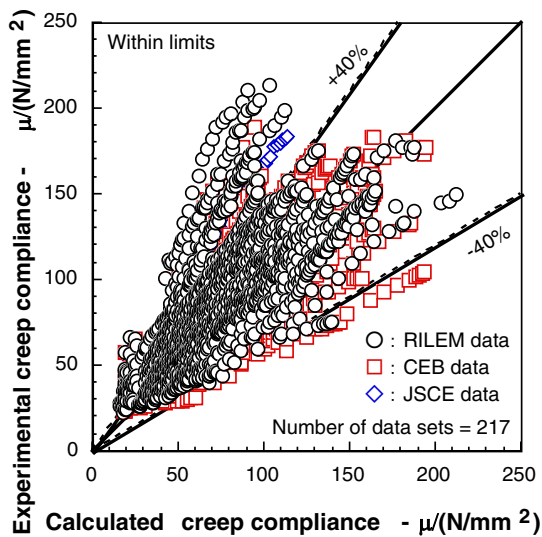


Figure 15 Precision of Model B3

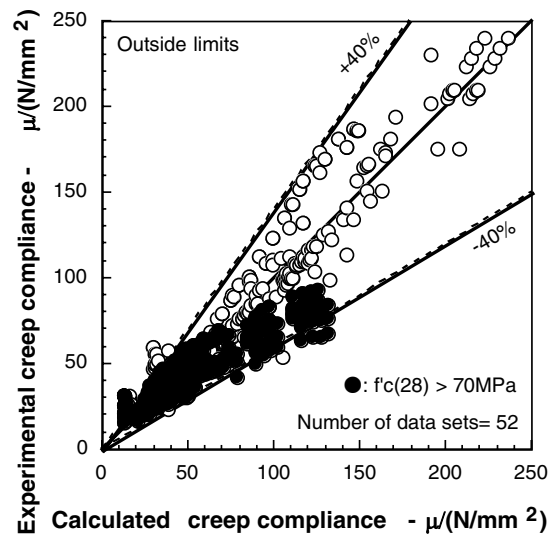


Figure 16 Precision of Model B3

Figure 17 compares experimental creep data with predictions by model GZ for data within the applicable range of model GZ. Model GZ tends to underestimate creep even for data within the applicable range. On the other hand, Figure 18 shows a similar comparison for data that is out of model GZ's applicable range. Symbol ● represents creep data for concrete whose strength at 28 days is above 70 N/mm². Symbol □ represents creep data for concrete for which drying began within 2 days. From this figure, it is clear that model GZ tends to overestimate creep strain when the concrete strength is high or the first application of loading is early. Despite that, the accuracy of model GZ is as good as any of the others.

All the models are able to predict creep to an accuracy of $\pm 40\%$, and it is clear that each prediction equation offers reasonable predictions of creep from the range of concrete strength from normal to high. However, in general, the prediction equations for creep are more complicated than those for shrinkage strain.

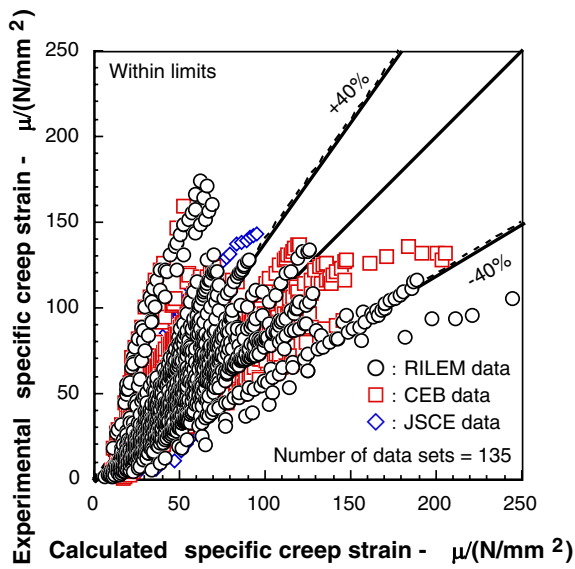


Figure 17 Precision of Model GZ

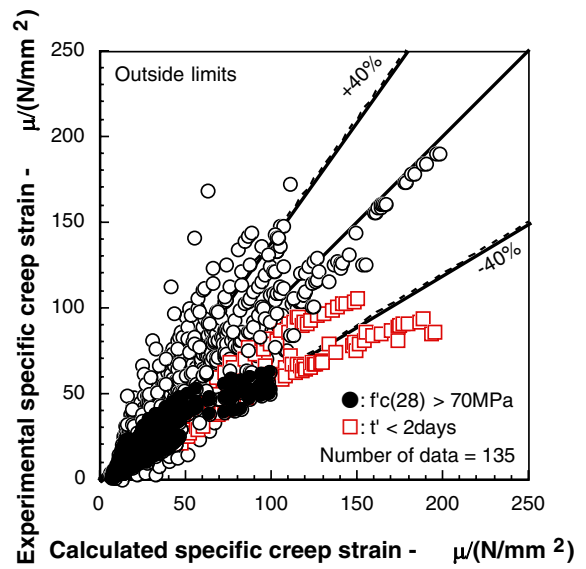


Figure 18 Precision of Model GZ

3. PROPOSED NEW SHRINKAGE PREDICTION EQUATION

3.1 Effect of concrete strength on ultimate shrinkage strain

Figure 19 shows the relationship between ultimate shrinkage strain and compressive strength at the start of drying. By regression, the development of shrinkage strain with time fits the hyperbola expressed by equation (3).

$$\varepsilon_{sh}(t, t_0) = \frac{\varepsilon_{sh\infty} \cdot (t - t_0)}{\beta + (t - t_0)} \quad (3)$$

Where, $\varepsilon_{sh\infty}$: ultimate shrinkage strain (μ), β : the term representing development of shrinkage strain, t : current age of concrete (days), t_0 : the start of drying (days).

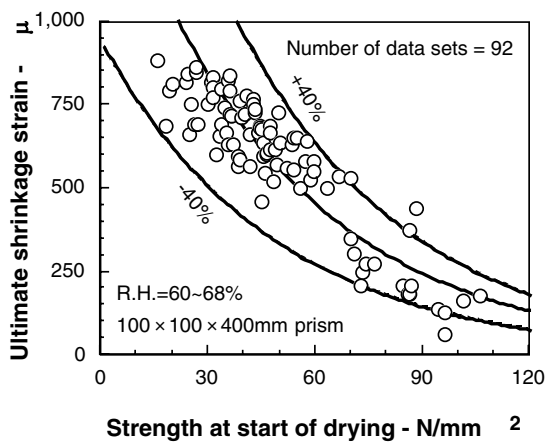


Figure 19 Relationship between ultimate shrinkage and concrete strength

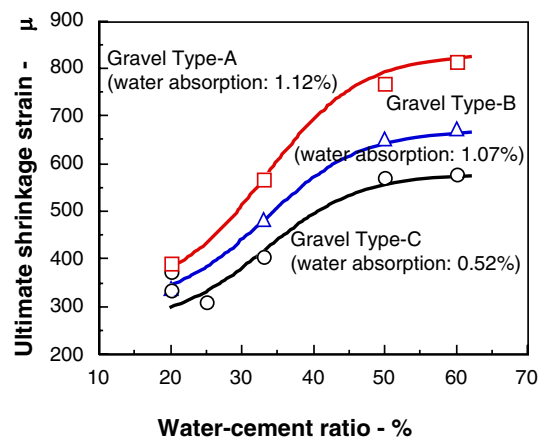


Figure 20 Relationship between ultimate shrinkage and W/C

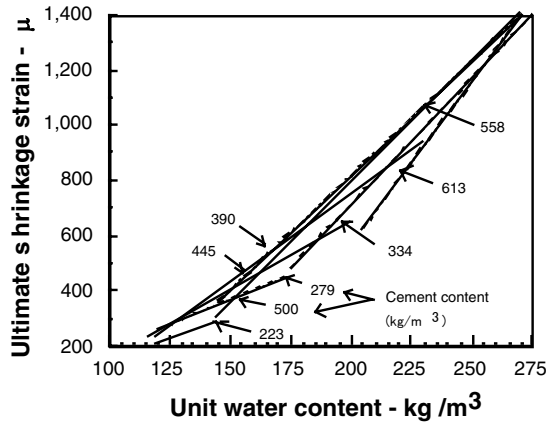


Figure 21 Effect of cement and water content on ultimate shrinkage

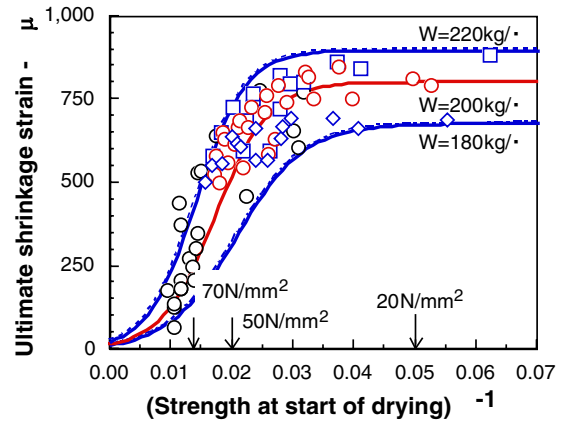


Figure 22 Relationship between ultimate shrinkage and concrete strength

As this makes clear, the greater the concrete strength at start of drying, the lower the ultimate shrinkage strain. When the relationship between ultimate shrinkage strain $\epsilon_{sh\infty}$ and the concrete strength at the start of drying is fitted to the hyperbola, every data point $\epsilon_{sh\infty}$ is within $\pm 40\%$ of the value on the curve. Many conventional prediction equations make use of this fitting [10][11]. However, as is clear from the results shown in Figure 20, the effect of concrete strength on ultimate shrinkage strain is small when the range of water-cement ratio is between 50% and 60%, that is, when the concrete strength is low. This result is independent of the type of gravel used.

Other investigations have also found the same result. Figure 21 shows the effect of water content on the ultimate shrinkage strain of normal-strength concrete [12]. It is clear from this figure that the effect of water content on ultimate shrinkage strain is much higher than that of water-cement ratio.

The horizontal axis of Figure 22 is the inverse of concrete strength at the start of drying. When concrete strength is less than 50 N/mm², the effect of strength is very small and the effect of water content is much greater. The results given in both Figures 21 and 22 were collected from not only normal concrete, but also concrete containing a wide range of water contents in order to investigate the effect of concrete mix proportion. We can conclude that the effect of water content on ultimate shrinkage strain depends on concrete strength, and that the effect of concrete strength on ultimate shrinkage strain is much higher than that of water content when the concrete strength is high.

This situation makes it very difficult to establish a shrinkage prediction equation that takes full account of all these dependencies, since neither of the databases stores information on concrete strength at the start of drying, though the 28-day strength was collected. For this reason, a prediction equation for ultimate shrinkage strain $\epsilon_{sh\infty}$ based on 28-day strength was established. The relationship between ultimate shrinkage strain $\epsilon_{sh\infty}$ and age at the start of drying is expressed by equation (4).

$$\epsilon_{sh\infty} = \frac{\epsilon_{sh\rho}}{1 + \varphi \cdot t_0} \quad (4)$$

Where, $\epsilon_{sh\rho}$, φ : the optimal values obtained by regression, t_0 : start of drying (days); however, $t_0=98$ when $t_0>98$.

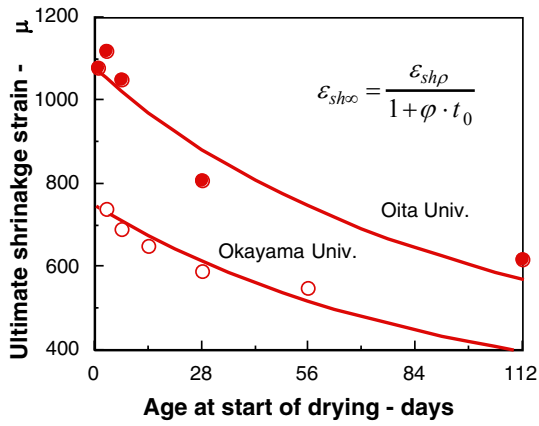


Figure 23 Effect of start of drying

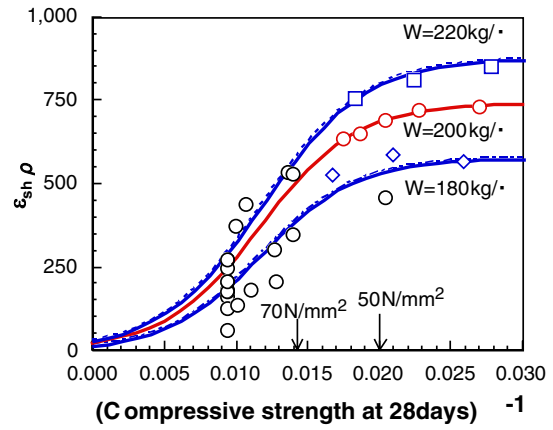


Figure 24 $\varepsilon_{sh\rho}$ and concrete strength

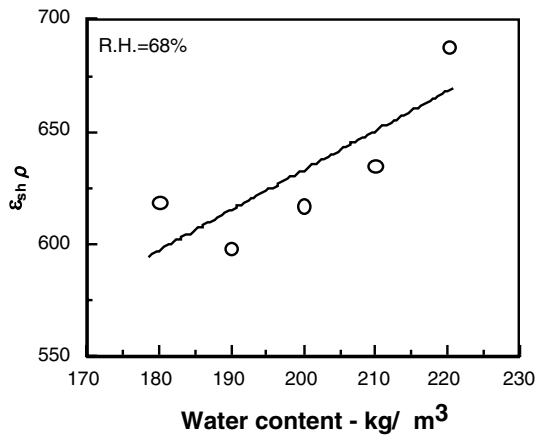


Figure 25 $\varepsilon_{sh\rho}$ and water content

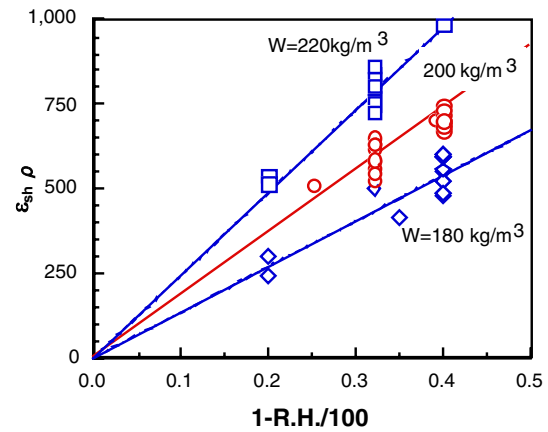


Figure 26 $\varepsilon_{sh\rho}$ and relative humidity

Figure 23 shows a regression example for the relationship between ultimate shrinkage strain $\varepsilon_{sh\infty}$ and age at the start of drying. It is clear that equation (4) expresses the relation well.

Figure 24 shows the relationship between $\varepsilon_{sh\rho}$ in equation (4) and the 28-day compressive strength. This demonstrates that $\varepsilon_{sh\rho}$ can be expressed by a single curve as long as the water content of the concrete is constant. The curves in Figure 24 were drawn using equation (5).

$$\varepsilon_{sh\rho} = \frac{C_{\rho 3}}{1 + C_{\rho 1} \exp\left(-\frac{C_{\rho 2}}{f'_c(28)}\right)} \quad (5)$$

Where, $C_{\rho 1}$, $C_{\rho 2}$, $C_{\rho 3}$: the optimal value decided by regression.

Figure 25 shows the relationship between $\varepsilon_{sh\rho}$ in equation (4) and water content in the case of normal-strength concrete whose 28-day strength is less than 40 N/mm². Further, Figure 26 shows the relationship between $\varepsilon_{sh\rho}$ and relative humidity of the atmosphere. Both relationships can be regarded as linear. Equation (6) is derived from this finding. The coefficients in this equation were obtained by regression from experimental data.

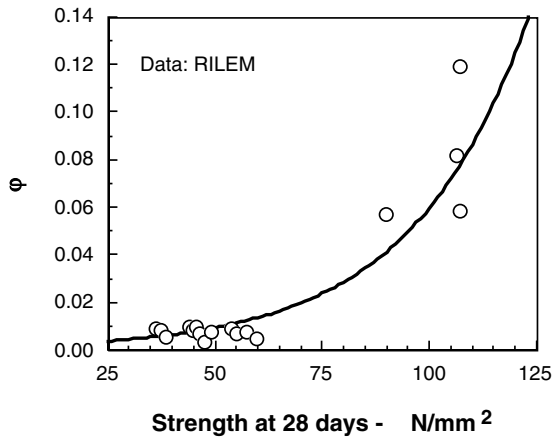


Figure 27 ϕ and concrete strength

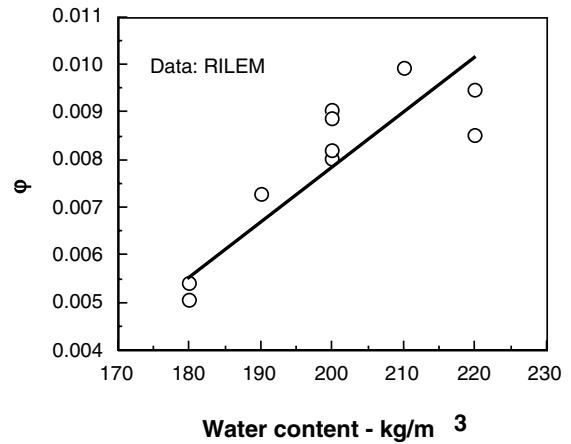


Figure 28 ϕ and water content

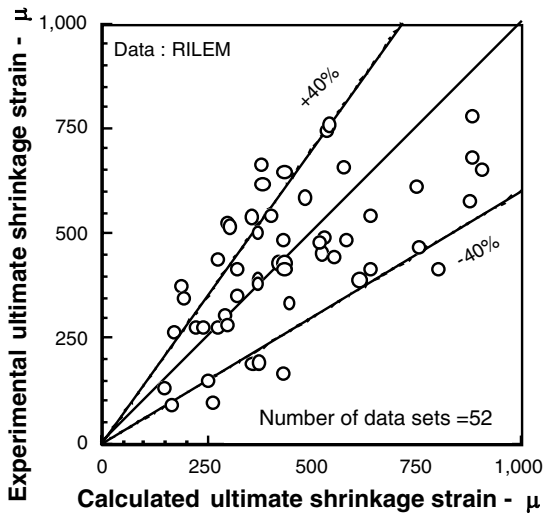


Figure 29 Precision of new model for ultimate shrinkage strain

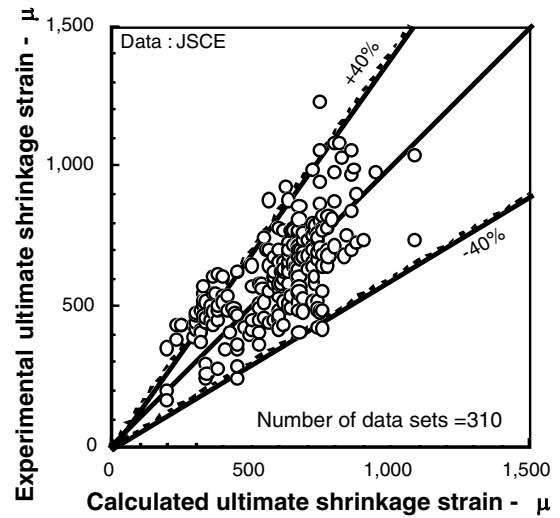


Figure 30 Precision of new model for ultimate shrinkage strain

$$\varepsilon_{shp} = \frac{\alpha(1-h)W}{1 + 150 \exp\left\{-\frac{500}{f'_c(28)}\right\}} \quad (6)$$

Where, α : coefficient depending on the type of cement, h : relative humidity as a decimal, W : water content (kg/m^3), $f'_c(28)$: 28-day concrete strength in compressive mode. When Japanese normal Portland cement is used, α is equal to 11.

Figure 27 shows the relationship between factor ϕ in equation (4) and 28-day concrete strength. As is clear from this figure, the greater the concrete strength at 28 days, the higher the factor ϕ . Factor ϕ is also affected by the water content of concrete, as shown in Figure 28, with the relationship between the two being linear. This understanding leads to the following equation (where the coefficients were obtained by regression from experimental data):

$$\phi = 10^{-4} \{15 \exp(0.007 f'_c(28)) + 0.25W\} \quad (7)$$

Where, $f'_c(28)$: concrete compressive strength at 28 days, W : water content (kg/m^3).

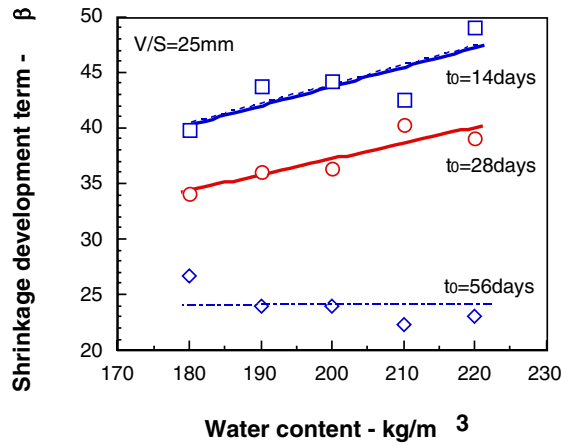


Figure 31 β and water content

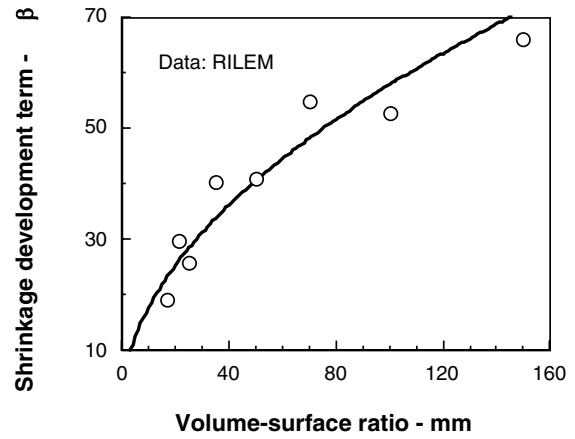


Figure 32 β and volume surface ratio

The vertical axes of both Figure 29 and Figure 30 are the experimental values of ultimate shrinkage strain. The horizontal axes are the calculated ultimate shrinkage strain using equations (4), (5), (6), and (7). The data in Figure 29 are from the European database, while those in Figure 30 are from the Japanese one. In equation (6), the coefficient α for the type of cement is set as follows: Japanese normal Portland cement and slow-hardening Portland cement: $\alpha=11$, Japanese rapid-hardening cement: $\alpha=15$, European early hardening and high-strength cement: $\alpha=11$, European normal and rapid-hardening cement: $\alpha=10$, European slow-hardening cement: $\alpha=8$. These values of coefficient α were obtained by regression from the experimental data. In fact, coefficient α also includes the effect of aggregate types used in different countries and other factors in addition to the concrete type.

It is clear from the figures presented here that the difference between experimental ultimate shrinkage strains and shrinkage strains calculated using equations (4), (5), (6), and (7) is mostly within $\pm 40\%$, and that the proposed prediction equation for ultimate shrinkage strain is very accurate.

3.2 Development of shrinkage strain

Figure 31 plots coefficient β for the development of shrinkage strain against concrete water content. The relationship is linear, and the effect of water content on β is small when the start of drying is late; that is, at 56 days. On the other hand, Figure 32 plots the volume surface ratio of the specimen against coefficient β . The greater the volume surface ratio of specimen, the bigger β . These findings are expressed by the following equation:

$$\beta = \left(\frac{C_{\beta 1}}{1 + C_{\beta 2} \cdot t_0} \cdot W + C_{\beta 3} \right) \cdot (V/S)^{C_{\beta 4}} \quad (8)$$

Where, W : water content (kg/m^3), V/S : volume surface ratio of the specimen (mm), $C_{\beta 1}$, $C_{\beta 2}$, $C_{\beta 3}$, and $C_{\beta 4}$: coefficients obtained by regression.

Using regression to obtain coefficient $C_{\beta 3}$ yields zero. The following equation was obtained.

$$\beta = \frac{4W\sqrt{V/S}}{100 + 0.7t_0} \quad (9)$$

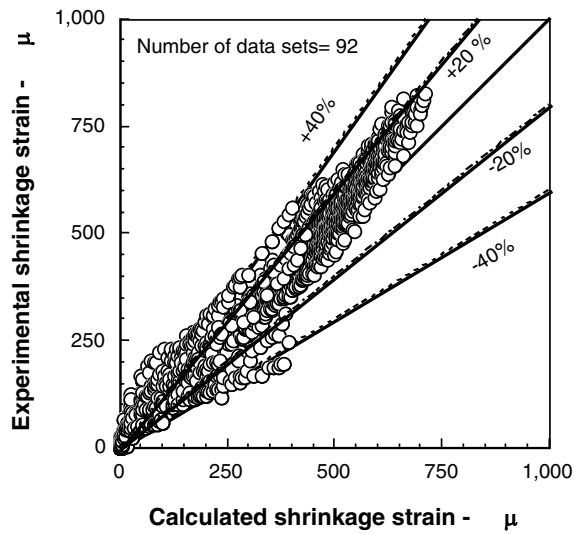


Figure 33 Precision of new prediction equation for shrinkage

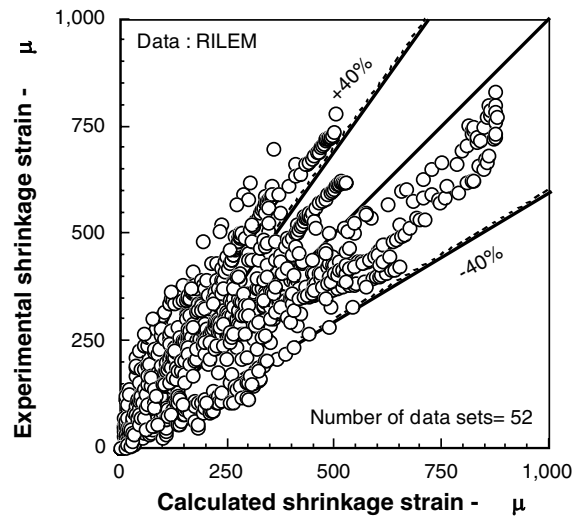


Figure 34 Precision of new prediction equation for shrinkage

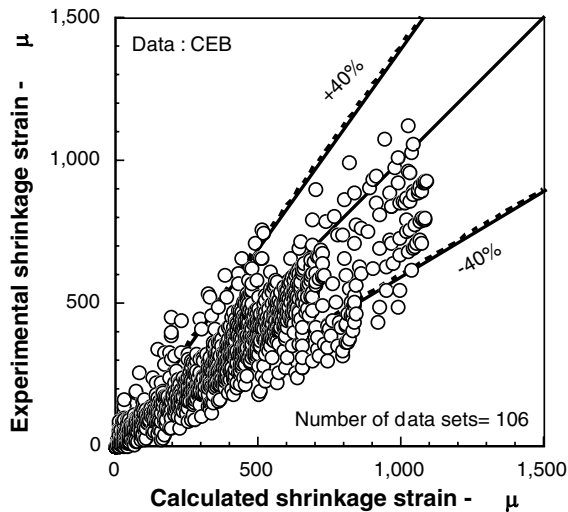


Figure 35 Precision of new prediction equation for shrinkage

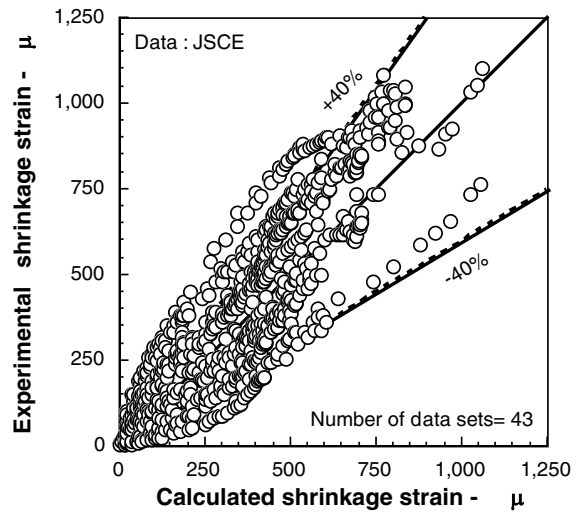


Figure 36 Precision of new prediction equation for shrinkage

3.3 Accuracy of proposed new prediction equation for shrinkage strain

Figures 33 to 36 compare the experimental shrinkage strain with values calculated using the new prediction equation proposed in this study, as discussed above. Overall, the discrepancy between measured and calculated values is within approximately $\pm 40\%$, so the proposed prediction equation is very accurate and applicable to a wide range of concrete strengths from normal to high-strength concrete.

4. PROPOSED NEW CREEP PREDITION EQUATION

4.1 Effect of concrete strength on ultimate creep

Figure 37 shows the relationship between ultimate specific creep and compressive strength at initial load application. By regression, the development of specific creep with time fits the hyperbola expressed by equation (10).

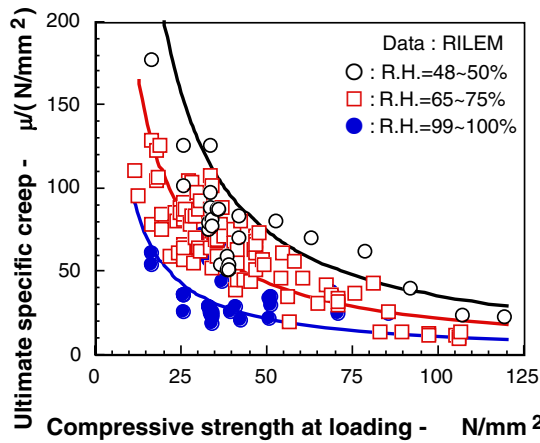


Figure 37 Relationship between ultimate creep and compressive strength

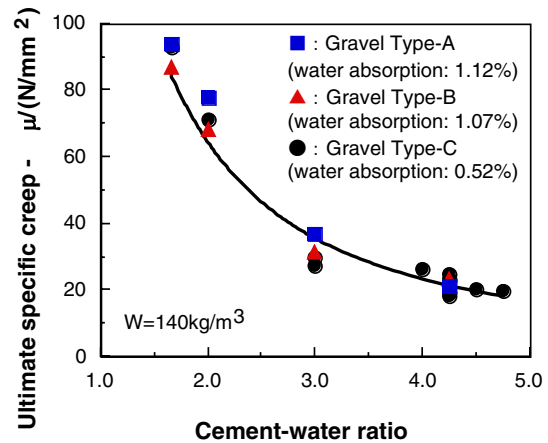


Figure 38 Relationship between ultimate creep and cement water ratio

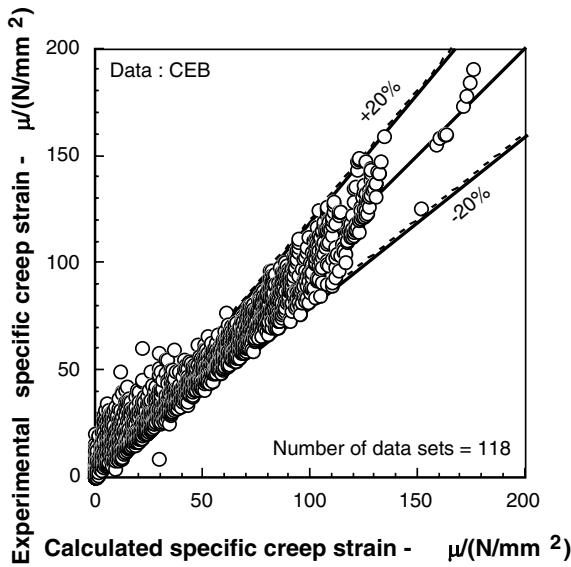


Figure 39 Accuracy when fitted to hyperbola

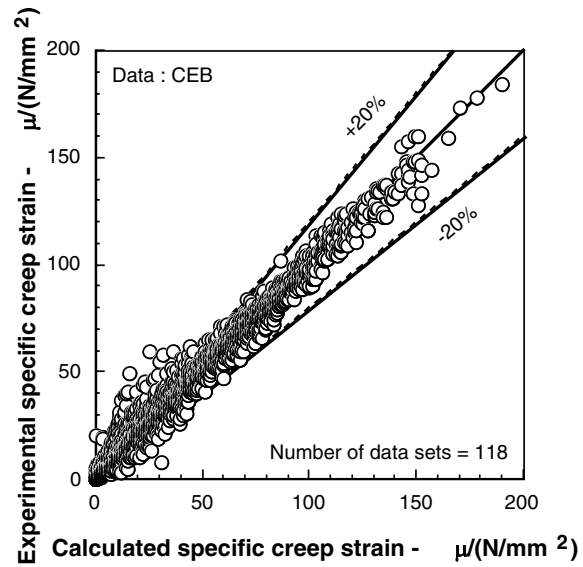


Figure 40 Accuracy when fitted to logarithmic curve

$$Cr(t, t') = \frac{Cr_{\infty} \cdot (t - t')}{\beta_{cr} + (t - t')} \quad (10)$$

Where, Cr_{∞} : ultimate specific creep ($\mu/N/mm^2$), β_{cr} : term representing the development of specific creep, t: current age of concrete (days), t': time at initial load application (days).

This figure clearly shows that the greater the concrete strength, the smaller the ultimate specific creep. The variance from average is also small at high concrete strengths. The same result was obtained from an experiment with a different type of gravel. Figure 38 shows that the ultimate specific creep becomes small when the water-cement ratio is small and concrete strength is high.

4.2 Development of creep

Figure 39 shows the results of fitting the specific creep to the hyperbola in equation (10). Similarly, Figure 40 shows the results of fitting specific creep to the logarithmic equation (11).

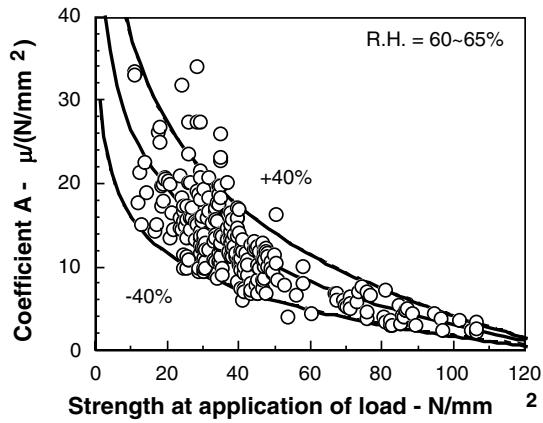


Figure 41 Relationship between coefficient A and compressive strength

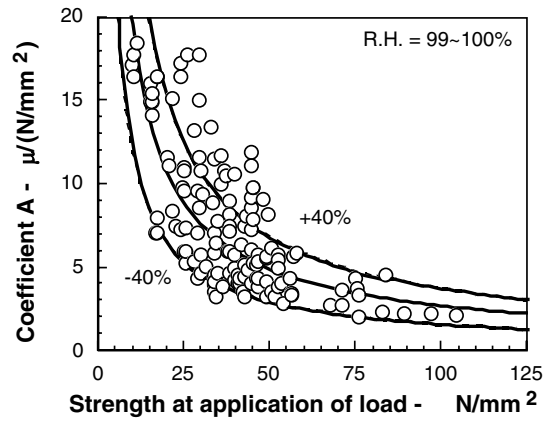


Figure 42 Relationship between coefficient A and compressive strength

$$Cr(t, t') = A \log_e(t - t' + 1) \quad (11)$$

Where, A: coefficient obtained by regression, t: age of concrete (days), t': age at initial load application (days).

The discrepancy between experimental values of specific creep and the hyperbolic and logarithmic curves fitted to specific creep by regression is basically within $\pm 20\%$. However, dispersion increases as time passes when the hyperbola is used for regression. On the other hand, when the logarithmic curve is used, the discrepancy with experimental data is large at an early stage. However, at later times, the regressed value fits the experimental data more closely. More importantly, just one coefficient is required to express the development of specific creep when the logarithmic curve is. It is thus very simple and convenient to establish a creep prediction equation.

Figures 41 and 42 show the relationship between coefficient A in equation (11) and concrete strength at initial load application. Figure 41 is for data measured at relative humidity levels between 60% and 65%. In Figure 42, on the other hand, the data were measured at relative humidity levels over 99%. It is clear from these figures that the relationship between coefficient A and concrete strength can be expressed by hyperbola. The lines fitted to the data in these figures are based on equation (12).

$$A = \frac{C_\alpha}{C_\beta + f'_c(t)} \quad (12)$$

Where, C_α , C_β : coefficients obtained by regression, $f'_c(t)$: concrete compressive strength at initial load application (N/mm²).

Figure 43 is a plot of coefficient A in equation (11) against the relative humidity of the atmosphere. The relationship is clearly linear. The relationship between coefficient A and water content is also linear, as seen in Figure 44. Equation (13) expresses this situation; when the relative humidity is 100%, then $h=1$ and the equation becomes that for basic creep. Thus, equation (13) separates the development of drying creep from the phenomenon of basic creep.

$$A = \frac{C_{drying} \cdot W(1-h)}{\varphi_{drying} + f'_c(t)} + \frac{C_{basic}}{\varphi_{basic} + f'_c(t)} \quad (13)$$

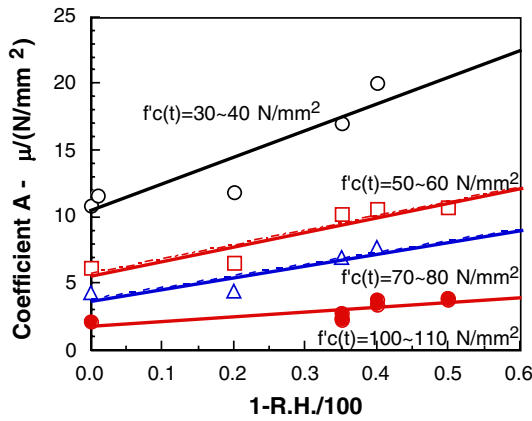


Figure 43 Relationship between coefficient A and relative humidity

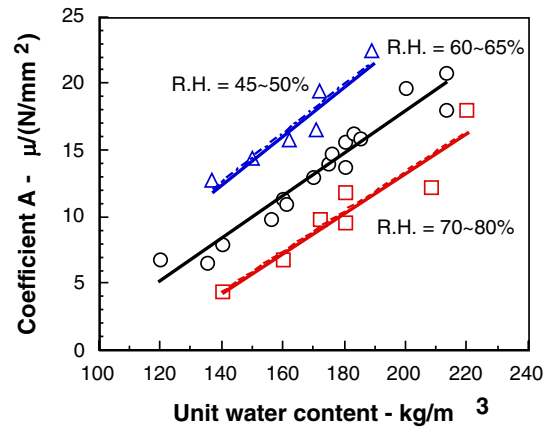


Figure 44 Relationship between coefficient A and water content of concrete

Where, C_{basic} , C_{drying} , φ_{basic} , φ_{drying} : coefficients obtained by regression, h : relative humidity as a decimal, W : water content (kg/m^3), $f'_c(t)$: compressive concrete strength (N/mm^2).

Obtaining every coefficient in equation (13) by regression shows that φ_{basic} is almost the same as φ_{drying} . The following equation can be derived as a consequence:

$$A = \frac{4W(1-h) + 350}{12 + f'_c(t)} \quad (14)$$

Equation (14) is obtained by regression using the many data given in Figure 2. Factors with little influence were eliminated. For example, the last JSCE model includes the effect of specimen size and shape. However, the new creep prediction equation proposed in this study does not include this influence because regression showed it to be small. Figure 45 shows the effect of volume surface ratio of the specimen on the predicted ultimate specific creep by model CEB and the JSCE model. The predicted value at a volume surface ratio of 100 mm is just 1.2 times bigger than that for a ratio of 1,000 mm, even when model CEB is used. This difference is even smaller when the last JSCE model is used. Models B3 and GZ include the effect of specimen size in the factor for creep development. This factor was excluded from the new creep prediction equation for the purpose of simplification.

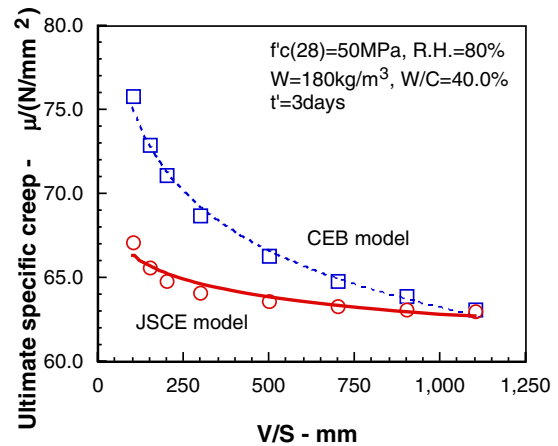


Figure 45 Relation between ultimate creep and volume surface ratio

4.3 Accuracy of proposed new prediction equation for specific creep

Figures 46 to 49 compare experimental measurements of specific creep with calculated values obtained by the new prediction equation proposed in this study. The discrepancy between measured values and predictions is generally within $\pm 40\%$, so the proposed prediction equation is very accurate and applicable to a wide range of concrete strengths from normal to high. The new

equation is extremely simple, yet its accuracy is as good as that of the major conventional equations.

5. NEW PREDICTION EQUATIONS PROPOSED IN THIS STUDY

To summarize, the newly proposed prediction equations for drying shrinkage are as follows:

$$\epsilon_{sh}(t, t_0) = \frac{\epsilon_{sh\infty} \cdot (t - t_0)}{\beta + (t - t_0)} \tag{15}$$

$$\epsilon_{sh\infty} = \frac{\epsilon_{sh\rho}}{1 + \eta \cdot t_0} \tag{16}$$

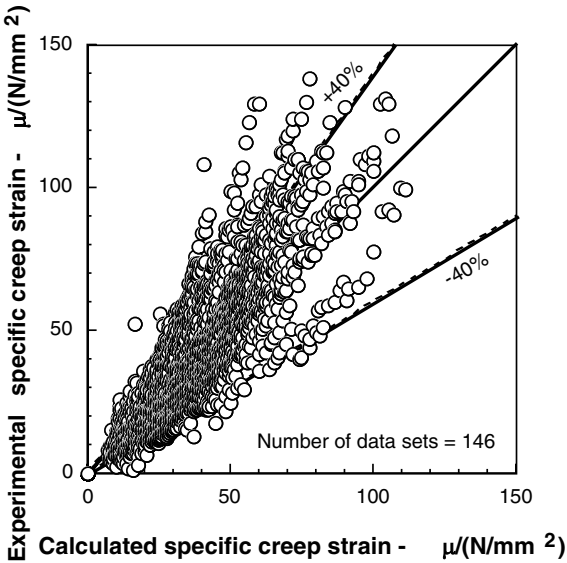


Figure 46 Precision of proposed model

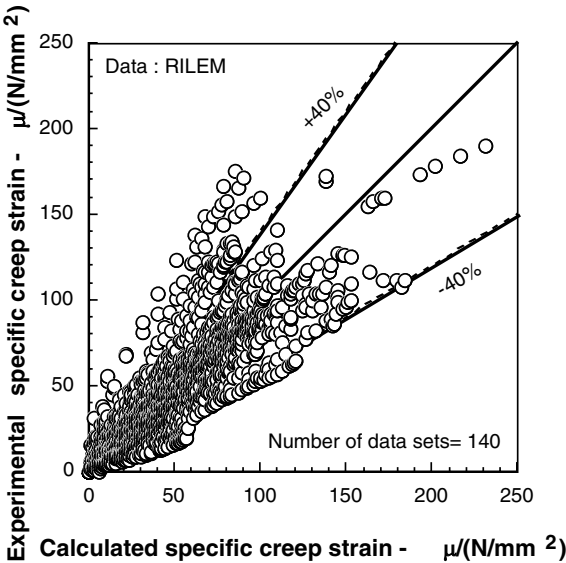


Figure 47 Precision of proposed model

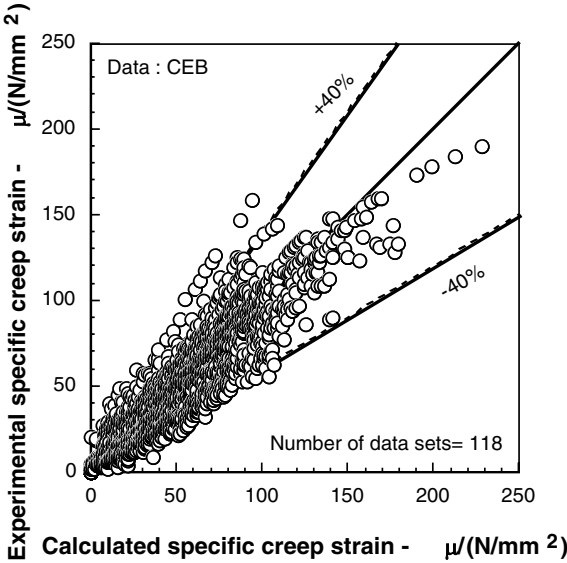


Figure 48 Precision of proposed model

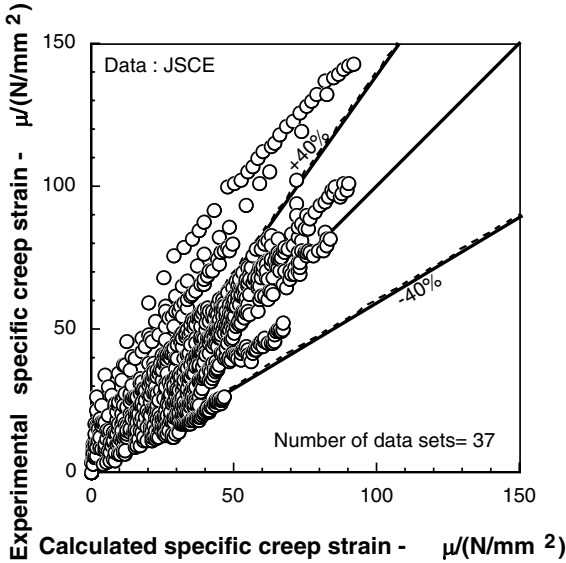


Figure 49 Precision of proposed model

$$\varepsilon_{shp} = \frac{\alpha(1-h)W}{1 + 150 \exp\left\{-\frac{500}{f'_c(28)}\right\}} \quad (17)$$

$$\eta = 10^{-4} \{15 \exp(0.007 f'_c(28)) + 0.25W\} \quad (18)$$

$$\beta = \frac{4W\sqrt{V/S}}{100 + 0.7t_0} \quad (19)$$

Where $\varepsilon_{sh}(t, t_0)$: drying shrinkage strain (μ), t, t_0 : current age and age at drying (days), when age at drying > 98 days, $t_0=98$. $f'_c(28)$: compressive strength at 28 days (N/mm^2) ($f'_c(28) < 120 N/mm^2$), h : relative humidity of atmosphere ($0.4 < h < 0.9$), W : unit water content ($130 < W < 230 kg/m^3$), V/S : volume surface ratio of specimen ($100 < V/S < 1,000 mm$), α : factor accounting for cement type (Japanese data: $\alpha = 11$ for normal cement and $\alpha = 15$ for rapid-hardening cement; Western data: $\alpha = 10$ for normal Portland cement and $\alpha = 8$ for slow-hardening cement).

The newly proposed prediction equation for creep is as follows:

$$Cr(t, t') = \frac{4W(1-h) + 350}{12 + f'_c(t')} \cdot \log_e(t - t' + 1) \quad (20)$$

Where, $Cr(t, t')$: specific creep ($\mu/N/mm^2$), h : relative humidity of the atmosphere ($0.4 < h < 0.9$), W : unit water content ($130 < W < 230 kg/m^3$), t' : time at initial load application (days) ($t' > 1$), $f'_c(t)$: compressive strength at age t (N/mm^2) ($f'_c(t) < 120 N/mm^2$).

6. CONCLUSION

New prediction equations for creep and shrinkage have been proposed and their accuracy investigated. The equations are based on a model established by statistical methods. The investigation results demonstrate that the proposed equations are able to predict concrete creep and shrinkage strain to a certain degree of accuracy.

The new shrinkage equation takes into account a number of influences. In particular, it takes account of the finding that the effect of water content on ultimate shrinkage strain depends on concrete strength, and that the effect of concrete strength on ultimate shrinkage strain is much higher than that of water content when the concrete strength is high.

The proposed creep equation is very simple, and specific creep can be predicted on the basis of just three items of data: compressive strength, relative humidity of the atmosphere, and water content. Despite this simplicity, it is able to predict the specific creep of concrete from normal strength to high strength with accuracy equivalent to that of typical conventional prediction equations.

The proposed prediction equations offer a simple design procedure for calculating creep and shrinkage using information available at the design stage.

References

[1] abc, edf: dog cat pen abc, abifdasd fdsafda fdsadas. Fdsafdsa fclassdf ise, dfasdfa fdasfda, fdsafdf dsaf fdsafa fda, 2002

- [2] ACI Committee 209: Prediction of creep and shrinkage, and temperature effects on concrete structures, American Concrete Institute Special Publication No.76, 1982.
- [3] JSCE: Standard specification for design and construction of concrete and structures, 1996.
- [4] RILEM TC 107 Subcommittee 5: Database on creep and shrinkage tests - 3.0, 1999.
- [5] Dilger, W. H.: Private communication.
- [6] JSCE committee 308: Concrete shrinkage and creep, Concrete Engineering Series, N0.24, pp.56~93, 1997 (in Japanese).
- [7] Comite Euro-International du Beton: CEB-FIP MODEL CODE 1990 (DESIGN CODE), Thomas Telford, pp.52~65, 1998.
- [8] Bazant, Z. P. and Baweja, S.: Creep and shrinkage prediction model for analysis and design of concrete structures - Model B3, Materials and Structures, RILEM, Paris, France, Vol. 28, pp.357~365, 1995.
- [9] Gardner, N. J.: Design Provisions for Shrinkage and Creep of Concrete, Proceedings of International Conference on Engineering Material, Ottawa, Canada, Vol.1, pp.647~657, 1997.
- [10] CEB-FIP: International Recommendations for the Design and Construction of Concrete Structures - Principles and Recommendations, Comite Europeen du Beton - Federation Internationale de la Precontrainte, FIP Sixth Congress, Prague, June 1970; published by Cement and Concrete Association: London, 1970.
- [11] Bazant, Z. P. and Panula, L.: Simplified prediction of concrete creep and shrinkage from strength and mix, Structural Engineering Reports No.78-10/6405, Department of Civil Engineering, Northwestern University, Evanston, Illinois, pp.24, Oct. 1978.
- [12] Kiyoshi Okada, Toyoki Akashi, and Wataru Koyanagi, Construction Materials for Civil Engineering, Kokumin Kagaku-sya, p.193, 1998 (in Japanese).